THE ASTROPHYSICAL JOURNAL, 506:647–657, 1998 October 20

THE DIFFERENCE BETWEEN THE NARROW-LINE REGIONS OF SEYFERT 1 AND SEYFERT 2 GALAXIES

HENRIQUE R. SCHMITT[1]
Departmento Astronomia, IF-Universidade Federal do Rio Grande do Sul, CP 15051, CEP 91501-970, Porto Alegre, RS, Brazil; schmitt@if1.if.ufrgs.br
Received 1997 August 25; accepted 1998 June 1

ABSTRACT

This paper presents a comparative study of emission-line ratios of the narrow-line regions (NLRs) of Seyfert 1 and Seyfert 2 galaxies. It includes a literature compilation of the emission-line fluxes [O II] λ3727, [Ne III] λ3869, [O III] λ5007, and [Ne V] λ3426 as well as 60 μm continuum flux, for a sample of 52 Seyfert 1 and 68 Seyfert 2 galaxies. The distribution of the emission-line ratios [O II]/[Ne III] and [O II]/[Ne V] shows that Seyfert 1 and Seyfert 2 galaxies are statistically different: Seyfert 1 galaxies have smaller values than Seyfert 2 galaxies, indicating a higher excitation spectrum. These and other emission-line ratios are compared with sequences of models that combine different proportions of matter and ionization-bounded clouds and also with sequences of models that vary only the ionization parameter. This comparison shows that the former models better reproduce the overall distribution of emission-line ratios, indicating that Seyfert 1 galaxies have a smaller number of ionization-bounded clouds than Seyfert 2 galaxies. This difference, together with other results available in the literature, are interpreted from the point of view of four different scenarios. The most likely scenario assumes that Seyfert 1 galaxies have smaller NLRs than Seyfert 2 galaxies, possibly due to a preferential alignment of the torus axis close to the host galaxy plane axis in Seyfert 1 galaxies.

Subject headings: galaxies: Seyfert — galaxies: active — galaxies: nuclei

1. INTRODUCTION

The observation of broad polarized lines in the spectrum of the Seyfert 2 galaxy NGC 1068 (Antonucci & Miller 1985) showed that Seyfert 2 galaxies can be Seyfert 1 galaxies where the direct view of the central engine is blocked. This is the basis for the unified model of active galactic nuclei (AGNs), which assumes that objects of different activity classes, such as Seyfert 1 and Seyfert 2 galaxies, are the same kind of object surrounded by a dusty molecular torus. The orientation of this torus relative to the line of sight determines whether the AGN is observed as a broad-line object (Seyfert 1), when the nuclear engine is seen through the torus opening, or as a narrow-line object (Seyfert 2), when our view of the central engine and consequently of the broad lines is blocked by the torus.

Several pieces of observational evidence supporting this scenario have been obtained during the last decade, the strongest being the observation of polarized broad emission lines in the spectrum of several Seyfert 2 galaxies (Antonucci & Miller 1985; Miller & Goodrich 1990; Kay 1994; Tran 1995). The observation of collimated radiation escaping the nuclear region of Seyfert 2 galaxies, seen as conelike emission-line regions (Pogge 1988a, 1988b, 1989; Schmitt, Storchi-Bergmann, & Baldwin 1994; Schmitt & Storchi-Bergmann 1995 and references therein) or linear radio structures (Ulvestad & Wilson 1984a, 1984b, 1989), also suggests that the direct view of the central engine is blocked in these objects. More direct evidence for the obscuration of the central engine in Seyfert 2 galaxies comes from the analysis of X-ray spectra, which show large absorbing column densities in these objects (Mulchaey, Mushotzky, & Weaver 1992). In addition, the observation of H_2O masers very close to the nuclei of some Seyfert 2 galaxies, such as NGC 1068 and NGC 4258 (Miyoshi 1995; Gallimore 1996; Greenhill 1996), show the presence of large concentrations of molecular gas, hiding the central engine.

Recent papers, however, present some results suggesting that not only the orientation of the circumnuclear torus relative to the line of sight but also its orientation relative to the host galaxy may be important in AGN classification. It has been known since the work of Keel (1980) that there is a paucity of Seyfert 1 galaxies with edge-on hosts. This result was later confirmed by Maiolino & Rieke (1995) and Simcoe et al. (1997), who suggested that, in some cases, dust along a Seyfert 1 galaxy disk may be responsible for the obscuration of the broad lines (making it appear as a Seyfert 2). Moreover, Schmitt et al. (1997) presented a comparison between the linear radio structures of Seyfert galaxies, with their host galaxy major axes. They found that the radio structures are more likely to be aligned close to the host galaxy plane axis in Seyfert 1 galaxies but can have any direction in Seyfert 2 galaxies, confirming the result of Maiolino & Rieke (1995). Another result that corroborates this scenario is the observation that the narrow-line regions (NLRs) of Seyfert 1 galaxies are usually much smaller than that of Seyfert 2 galaxies, when they are compared as if Seyfert 2 galaxies were observed pole-on, in the same way as the Seyfert 1 galaxies (Schmitt & Kinney 1996). The smaller Seyfert 1 NLRs can be understood if these objects have their torus axes preferentially aligned close to the host galaxy plane axis, where there is less gas to be ionized.

The above results show differences between the NLRs of Seyfert 1 and Seyfert 2 galaxies and point to older papers, where some other differences have also been detected. Heckman & Balick (1979) and Shuder & Osterbrock (1981) showed that the ratio [O III] λ4363/λ5007 is larger in Seyfert 1 than in Seyfert 2 galaxies. This result indicates that the [O III] zone of Seyfert 1 galaxies, when compared to Seyfert 2 galaxies, have larger temperatures and/or densities. Yee (1980) and Shuder (1980) showed that the emis-

[1] CNPq Fellow.

sion lines [O III], [O II], and [O I] are more luminous in Seyfert 2 galaxies than in Seyfert 1 galaxies of similar optical luminosity, consistent with the torus blocking part of the continuum light in Seyfert 2 galaxies. Shuder & Osterbrock (1981) and Cohen (1983) showed that the emission-line ratios [Fe VII]/Hβ and [Fe X]/Hβ are larger in Seyfert 1 than in Seyfert 2 galaxies, indicating that Seyfert 1 galaxies have higher excitation. Yet another interesting result was obtained by De Robertis & Osterbrock (1986 and references therein), who showed that the FWHMs of forbidden lines correlate well with the ionization potential in Seyfert 1 galaxies, but not with the critical density for deexcitation, while in Seyfert 2 galaxies the opposite is true. They have also showed that these lines have smaller FWHMs in Seyfert 1 galaxies than in Seyfert 2 galaxies, and that the [O I] line profiles show evidence of two components in Seyfert 2 galaxies, probably formed in two different regions.

This paper presents a compilation of literature data on the emission-line fluxes [O II] λ3727, [Ne III] λ3869, [Ne V] λ3426, and [O III] λ5007 (hereafter [O II], [Ne III], [Ne V], and [O III]), as well as 60 μm continuum fluxes, for a sample of 52 Seyfert 1 and 68 Seyfert 2 galaxies. These lines are used to compare the excitation of the NLR gas in Seyfert 1 and Seyfert 2 galaxies, through analysis of different emission-line ratios. A simple interpretation of the unified scheme would suggest that the spectrum of the NLRs of Seyfert 1 and Seyfert 2 galaxies should have similar degrees of excitation. However, as shown by the above papers, this may not be true. Effects such as the possible obscuration of parts of the NLR by the torus, or the smaller NLR size in Seyfert 1 galaxies, could influence the average NLR excitation in these two classes of objects.

This paper is organized in the following way. Section 2 presents the sample, the reasons for the choice of these emission lines, and a discussion of the possible selection effects. Section 3 shows the results of the comparison between Seyfert 1 and Seyfert 2 galaxies. Section 4 shows the comparison between the data and photoionization models and discusses possible interpretations of the results, while § 5 gives a summary.

2. THE DATA AND SELECTION EFFECTS

The usual way to analyze the gas excitation in galaxies is through the use of ratios between different emission-line fluxes. The most common approach is to use BPT diagrams (Baldwin, Phillips, & Terlevich 1981), which allow differentiation between Seyfert 2 galaxies, LINERs, and H II regions. These diagrams use emission-line ratios such as [O II]/[O III], [N II]/Hα, and [O III]/Hβ, which can be easily measured in Seyfert 2 galaxies. However, because of blending with broad lines, as is the case for Hβ and Hα + [N II], these lines cannot be easily measured in Seyfert 1 galaxies. Another problem is the difficulty of determining the internal reddening in Seyfert 1 galaxies, which can considerably influence the [O II]/[O III] ratio.

In order to avoid the above problems, a different set of emission lines, easily measurable in both Seyfert 1 and Seyfert 2 galaxies, is chosen. These lines are [O II] λ3727, [Ne III] λ3869, [Ne V] λ3426, and [O III] λ5007. They span a wide range in ionization potentials, are not blended with other lines (either broad or narrow), and, with the exception of [O III], they are close in wavelength, which minimizes scatter resulting from reddening effects and relative flux calibration errors. [Ne III] is of particular interest because its values for the ionization potential and the critical density for collisional deexcitation are very similar to those of [O III], implying that they may be formed in similar regions. In this way, the ratio [O II]/[Ne III] can be used in place of [O II]/[O III], with the advantage of being reddening free. For more details on the use of [Ne III] in diagnostic diagrams, see Rola, Terlevich, & Terlevich (1997).

The literature was searched for Seyfert 1 and Seyfert 2 galaxies with measured emission-line fluxes of the lines [O II], [Ne III], [Ne V], and [O III]. We found 52 Seyfert 1 and 68 Seyfert 2 galaxies, shown in Tables 1 and 2, respectively. These tables give the names of the objects, *B* magnitude, radial velocity, morphological type (de Vaucouleurs et al. 1991; Mulchaey 1994), the emission-line ratios [O II]/[Ne III], [O II]/[Ne V], [Ne III]/[Ne V], and [O II]/[O III], the *IRAS* 60 μm flux, the reference from which the emission-line ratios were obtained, and the aperture size used to observe the spectrum. Note that it was not possible to find [Ne V] and 60 μm flux, or occasionally morphological type, for all galaxies in the sample.

An important point about the data collection is that for every object, emission-line fluxes from two different references were never mixed. In addition, preference was given to data obtained with medium-size apertures (3″–7″), in order to include as much NLR emission as possible but also to avoid extremely large aperture sizes, which could include H II regions in the galaxy disk. The apertures given in Tables 1 and 2 were classified into three categories: S (small), corresponding to apertures smaller than 3″, M (medium), corresponding to apertures in the range 3″–7″, and L (large), corresponding to apertures larger than 7″.

The radial velocities and aperture sizes (in arcseconds) were used to calculate the metric aperture sizes, which correspond to the dimension of the aperture in the galaxy (in parsecs), calculated assuming $H_0 = 75$ km s^{-1} Mpc^{-1}. These values were calculated by taking the square root of the slit area, and in comparing the average metric aperture sizes for Seyfert 1 and Seyfert 2 galaxies, it was found that they have similar values, with means and 1 σ uncertainties of 1972 ± 1578 and 2008 ± 2101 pc, respectively. The Spearman rank test was used to compare the four emission-line ratios with the metric aperture sizes. These do not show any correlation, confirming that aperture effects are not a problem for the analysis.

Since the sample was obtained from the literature, rather than selected from an isotropic property, it is necessary to check if both Seyfert 1 and Seyfert 2 galaxies have similar intrinsic properties. First we checked to see whether Seyfert 1 and Seyfert 2 galaxies have similar luminosities and are not biased toward high-luminosity Seyfert 1 and low-luminosity Seyfert 2 galaxies, which could imply a larger flux of high excitation lines in Seyfert 1 galaxies. This test was made by comparing the 60 μm luminosities of the two groups of galaxies. Here it was assumed that the 60 μm luminosity is nuclear radiation absorbed by the circumnuclear torus and reradiated in the far-infrared, so it should scale with total luminosity. However, note that it can depend on the torus covering factor, which can differ for Seyfert 1 and Seyfert 2 galaxies. It should also be noted that the assumption that 60 μm luminosity scales with the nuclear luminosity must be taken with caution, since (as pointed out by Pier & Krolik 1992) the torus emission may be anisotropic even at 60 μm.

The results for this comparison are shown in Figure 1, where it can be seen that both groups have similar distributions, with the Kolmogorov-Smirnov (K-S) test showing

TABLE 1

SEYFERT 1 GALAXIES

Name	B	V_0 (km s^{-1})	Morphology	[O II]/[Ne III]	[O II]/[Ne V]	[Ne III]/[Ne V]	[O II]/[O III]	$F_{60\ \mu m}$ (Jy)	Reference	Aperture
NGC 1019	14.95	7290	SBbc	2.955	...	...	0.210	0.355	1	M
NGC 1566	13.17	1290	SABbc	2.375	...	...	0.255	14.71	2	S
NGC 3227	13.52	990	SABa pc	1.603	5.05	3.150	0.177	7.825	3	S
NGC 3516	12.40	2700	SB0	0.667	0.857	1.286	0.126	1.758	4	L
NGC 3783	13.43	2880	SBa	0.414	0.861	2.080	0.081	3.257	5	M
NGC 4051	12.65	600	SABbc	1.571	1.100	0.700	0.292	7.131	4	L
NGC 4151	11.85	900	SABab	1.087	1.880	1.729	0.096	...	6	S
NGC 4253	13.60	3810	SB0/a	0.952	1.111	1.167	0.053	4.026	7	M
NGC 4593	13.15	2610	SBb	0.782	1.165	1.490	0.170	3.052	5	M
NGC 5033	10.75	892	SAc	2.727	...	...	0.600	13.8	8	S
NGC 5548	13.73	5100	SA0/a	2.579	0.547	0.212	0.098	1.073	3	S
NGC 6814	14.21	1590	SABbc	1.443	0.988	0.685	0.115	5.517	5	M
NGC 6860	13.50	4470	SBb	2.556	...	...	0.343	0.954	9	S
NGC 7450	14.33	3120	SBa	2.115	1.170	0.553	0.128	...	7	M
NGC 7469	13.15	4830	SABa	2.310	...	...	0.164	25.87	5	M
Mrk 6	14.19	5610	SAB0$^+$	2.394	...	...	0.174	1.183	10	M
Mrk 42	15.28	7350	...	2.157	...	...	0.297	0.317	7	M
Mrk 79	14.02	6570	SBb	1.362	1.595	1.171	0.170	1.503	3	S
Mrk 279	14.46	9150	S0	3.224	...	...	0.427	1.255	3	S
Mrk 315	14.78	11820	S0/a pc	2.179	...	...	0.442	1.464	10	M
Mrk 359	14.22	5072	SB0	1.143	0.750	0.656	0.076	1.132	7	M
Mrk 372	14.81	9300	S0/a	2.046	...	...	0.253	0.303	10	M
Mrk 506	14.68	12900	SABa	3.136	...	...	0.153	...	3	S
Mrk 509	13.12	10650	E/S0	2.077	0.242	0.117	0.262	1.364	5	M
Mrk 595	14.69	8250	E/S0	1.769	...	...	0.230	...	11	M
Mrk 704	14.23	8730	Sa	0.509	0.348	0.684	0.082	0.364	3	S
Mrk 783	16.00	20000	...	3.167	...	...	0.296	0.31	7	M
Mrk 817	13.90	9600	S0/a pc	0.687	0.234	0.340	0.054	2.118	3	S
Mrk 841	14.85	10950	...	1.042	0.953	0.915	0.192	0.459	5	M
Mrk 871	14.80	10200	SB0	0.989	0.463	0.468	0.101	0.69	5	M
Mrk 896	14.61	7860	S?	1.543	0.679	0.440	0.152	0.513	5	M
Mrk 926	14.20	14400	Sa	2.133	5.818	2.727	0.312	...	12	S
Mrk 975	14.95	14730	S pec	0.541	0.338	0.625	0.063	0.8	3	S
Mrk 1018	14.30	12810	S0	1.636	...	...	0.180	...	13	S
Mrk 1239	14.39	5820	Compact	1.050	...	...	0.150	1.335	7	M
Mrk 1320	15.00	30900	SBb	3.482	...	...	0.409	0.218	5	M
IC 4218	14.40	5820	Sb-c	1.536	...	...	0.232	...	5	M
IC 4329a	13.66	4800	S0$^+$	1.2	...	...	0.028	2.03	14	S
MCG 8-11-11	14.00	6150	SBb-c	2	3.227	1.614	0.151	3.005	3	S
MCG−6-30-15	13.61	2340	E/S0	2.273	2.423	1.066	0.222	1.087	5	M
UM 146	14.50	5160	SAb	2.475	...	...	0.120	0.467	1	M
Fairall 51	14.10	4080	SBb	1.668	0.880	0.528	0.193	1.844	5	M
ESO 141-G55	13.60	11040	Sc	0.795	...	...	0.092	0.575	5	M
UGC 10683b	15.55	9200	...	1.421	0.231	0.163	0.145	0.479	5	M
TOL 0343-397	14.83	12900	E	1.692	...	...	0.321	0.24	15	L
TOL 1351-373	...	15500	...	1.476	1.594	1.080	0.107	0.45	5	M
TOL 1506.3-00	...	16200	...	2.039	2.676	1.312	0.204	...	5	M
TOL 20	...	7000	...	0.553	0.588	1.063	0.080	...	5	M
C 16.16	17.19	22864	...	2.3	3.286	1.429	0.217	...	16	S
E 1615+061	...	11370	...	2.789	6.092	2.185	0.301	...	5	M
H 1839-78	...	22200	...	0.778	0.348	0.447	0.162	...	5	M
IIIZw 77	...	10250	...	0.642	0.385	0.600	0.090	0.245	17	M

NOTE.—Morphological types were obtained from de Vaucouleurs et al. 1991 and Mulchaey 1994. The ninth column gives the references for the emission lines.

REFERENCES.—(1) Phillips, Charles, & Baldwin 1983; (2) Alloin et al. 1985; (3) Cohen 1983; (4) Anderson 1970; (5) Morris & Ward 1988; (6) Boksenberg et al. 1975; (7) Osterbrock & Pogge 1985; (8) Shuder 1980; (9) Lipari, Tsvetanov, & Macchetto 1993; (10) Koski 1978; (11) Ulvestad & Wilson 1983; (12) Durret & Bergeron 1988; (13) Osterbrock 1981; (14) Wilson & Penston 1979; (15) Terlevich et al. 1991; (16) Rodriguez-Ardila et al. 1996; (17) Ferland & Osterbrock 1986.

that two samples drawn from the same parent population would differ this much 44% of the time. Table 3 gives the numbers of Seyfert 1 and Seyfert 2 galaxies with 60 μm luminosities available, their mean values, standard deviations, and the K-S test probability. This table also gives information about other results from the K-S tests done below. The four emission-line ratios were also compared with the 60 μm luminosity, but the Spearman rank test did not show any correlation. It should be noted, however, that not all galaxies have *IRAS* 60 μm fluxes available; we have them for only 40 out of the 52 Seyfert 1 and 52 out of the 68 Seyfert 2 galaxies examined.

The second test checks whether the two groups have similar morphological types and are not biased toward Seyfert 2 galaxies in late-type galaxies. Late-type galaxies are more likely to have circumnuclear H II regions, which usually have much stronger [O II] than [Ne III] fluxes, which would make Seyfert 2 galaxies look like lower excita-

TABLE 2

Seyfert 2 Galaxies

Name	*B*	V_0 (km s^{-1})	Morphology	[O II]/[Ne III]	[O II]/[Ne V]	[Ne II]/[Ne V]	[O II]/[O III]	$F_{60\ \mu m}$ (Jy)	Reference	Aperture
NGC 424	14.12	3300	SB0/a	1.310	...	...	0.130	1.796	1	S
NGC 1068	10.83	1020	Sb	0.809	1.056	1.306	0.058	181.95	2	M
NGC 1229	14.00	10590	SBb pec	4.179	3.836	0.918	0.263	1.548	3	M
NGC 1358	13.05	3870	SAB0/a	4.253	...	...	0.387	0.378	4	L
NGC 1386	12.84	810	Sa/S0	2.810	...	...	0.177	5.396	4	L
NGC 1667	12.77	4472	Sc	5.182	...	...	0.371	5.952	3	M
NGC 2110	13.51	2130	SA0	4.300	...	...	0.430	4.129	5	S
NGC 2992	13.78	2250	Sa pec	4.623	...	...	0.319	6.760	6	L
NGC 3081	13.55	2160	SAB0/a	1.949	1.086	0.557	0.164	...	7	S
NGC 3281	14.02	3540	SAa	3.022	3.886	1.286	0.245	6.861	8	S
NGC 3393	12.40	3690	Sa	4.179	...	...	0.148	2.251	9	M
NGC 3786	13.74	2760	SABa pc	3.553	...	...	0.270	...	10	S
NGC 3982	11.70	10800	SABb	2.056	...	...	0.153	6.567	3	M
NGC 4074	14.44	6600	S0 pec	1.818	1.471	0.809	0.100	...	11	S
NGC 4388	11.76	2545	SAb	5.586	...	...	0.324	10.240	6	L
NGC 4507	13.54	3480	SBab	3.921	4.798	1.224	0.265	4.310	7	S
NGC 4941	12.23	870	SABab	4.079	...	...	0.257	1.378	4	L
NGC 4939	13.80	2910	SAbc	1.484	...	...	0.095	2.015	6	L
NGC 5135	13.35	3990	SBab	2.524	...	...	0.220	16.910	3	M
NGC 5256	13.42	8280	S0 pec	5.446	...	...	0.635	7.342	12	S
NGC 5347	12.70	2370	SBab	1.848	1.525	0.825	0.508	1.424	13	S
NGC 5506	14.38	1830	Sa pec	3.586	9.369	2.613	0.267	8.409	14	M
NGC 5643	13.60	990	SABc	1.844	1.895	1.028	0.152	19.490	14	M
NGC 5728	13.40	2790	SABa	2.453	5.257	2.143	0.156	8.163	3	M
NGC 6300	13.08	900	SBb	2.491	...	...	0.279	14.650	4	L
NGC 6890	14.02	2430	SAb	1.081	...	...	0.107	3.855	6	L
NGC 7130	13.87	4830	Sa pec	2.442	...	...	0.188	16.480	6	L
NGC 7314	13.11	1500	SABbc	2.401	2.290	0.954	0.139	3.736	14	M
NGC 7582	13.57	1560	SBab	1.745	6.584	3.772	0.258	49.100	15	M
NGC 7743	13.28	2040	SB0/a	1.871	...	...	0.595	0.791	4	L
Mrk 1	14.96	4800	SB0/a	1.491	3.286	2.204	0.137	2.531	2	M
Mrk 3	13.34	4110	E2 pec	2.351	...	...	0.164	3.770	2	M
Mrk 34	14.76	15450	S	3.000	...	...	0.220	0.809	2	M
Mrk 78	15.00	11145	E/S0	2.383	...	...	0.196	1.110	2	M
Mrk 176	14.61	8070	S0/a pc	1.111	...	...	0.108	0.694	2	M
Mrk 198	14.73	7170	SAB0 pc	4.370	...	...	0.351	0.624	2	M
Mrk 268	14.66	12300	Sa	4.410	...	...	0.535	1.381	2	M
Mrk 270	14.05	3090	SAB0	3.943	...	...	0.541	...	2	M
Mrk 348	13.90	4410	SA0/a	2.480	...	...	0.247	1.290	2	M
Mrk 423	14.29	9720	S0?	3.591	...	...	0.790	1.423	16	S
Mrk 463e	14.22	15150	S pec	3.231	...	...	0.210	2.184	11	S
Mrk 516	16.50	8519		3.765	...	...	0.640	1.325	16	S
Mrk 573	14.07	5130	SAB0	2.089	...	...	0.167	1.088	2	M
Mrk 609	14.12	10260	E/S0	1.545	3.333	2.157	0.170	2.550	16	S
Mrk 612	15.50	6206	SB0/a?	1.864	...	...	0.110	1.159	11	S
Mrk 622	14.40	6840	S0 pec	7.656	...	...	0.490	1.281	11	S
Mrk 1066	14.01	3540	SB0	4.211	...	...	0.320	10.98	10	S
Mrk 1193	16.50	9600	...	3.355	...	...	0.190	0.641	17	L
Mrk 1388	15.70	6390		0.473	...	...	0.048	0.174	18	S
IC 1515	14.80	6870	SBb	1.524	0.976	0.641	0.170	0.566	3	M
IC 5063	13.60	3300	SA0a pc	3.656	...	...	0.223	5.337	6	L
MCG−5-23-16	13.69	2280	S0	1.533	1.769	1.154	0.110	...	8	S
UM 16	17.00	17400	...	1.605	2.653	1.653	0.130	...	11	S
UM 82	17.88	15300	...	1.802	...	...	0.095	...	17	L
UM 85	17.29	12300	...	3.293	...	...	0.174	...	17	L
UM 103	17.00	13500	...	3.113	...	...	0.280	...	17	L
UM 293	16.40	16800	...	2.804	...	...	0.239	...	17	L
Fairall 4	15.10	15900	Sb	1.579	...	...	0.101	...	17	L
ESO 138-G1	14.31	2730	E/S0	2.219	1.426	0.643	0.193	...	19	M
ESO 103-G35	14.53	4050	S0?	5.651	...	...	0.365	2.314	14	M
TOL 0514-415	...	14700	...	4.154	...	...	0.300	...	17	L
TOL 0544-395	14.90	7500	S0	3.584	...	...	0.239	0.917	17	L
TOL 0611-375	...	11400	...	4.115	...	...	0.213	...	17	L
WAS 49a	...	18900	...	1.923	5.263	2.737	0.101	0.438	20	S
POX 52	17.20	...	...	3.509	8.000	2.280	0.288	...	21	M
IZw 92	15.20	11340	...	2.062	3.448	1.672	0.200	1.313	11	S
IIIZw 55	15.40	7507	...	1.928	...	...	0.172	0.867	2	M
VZw 317	15.77	10200	...	1.571	...	...	0.660	...	16	S

Note.—Morphological types were obtained from de Vaucouleurs et al. 1991 and Mulchaey 1994.

References.—(1) Cohen 1983; (2) Koski 1978; (3) Phillips et al. 1983; (4) Storchi-Bergmann & Pastoriza 1989; (5) Shuder 1980; (6) Storchi-Bergmann, Bica, & Pastoriza 1990; (7) Durret & Bergeron 1986; (8) Durret & Bergeron 1988; (9) Diaz, Prieto, & Wamsteker 1988; (10) Goodrich & Osterbrock 1983; (11) Shuder & Osterbrock 1981; (12) Osterbrock & Dahari 1983; (13) Gonzalez Delgado & Perez 1996; (14) Morris & Ward 1988; (15) Ward et al. 1980; (16) Osterbrock 1981; (17) Terlevich et al. 1991; (18) Osterbrock 1985; (19) Alloin et al. 1992; (20) Moran et al. 1992; (21) Kunth, Sargent, & Bothum 1987.

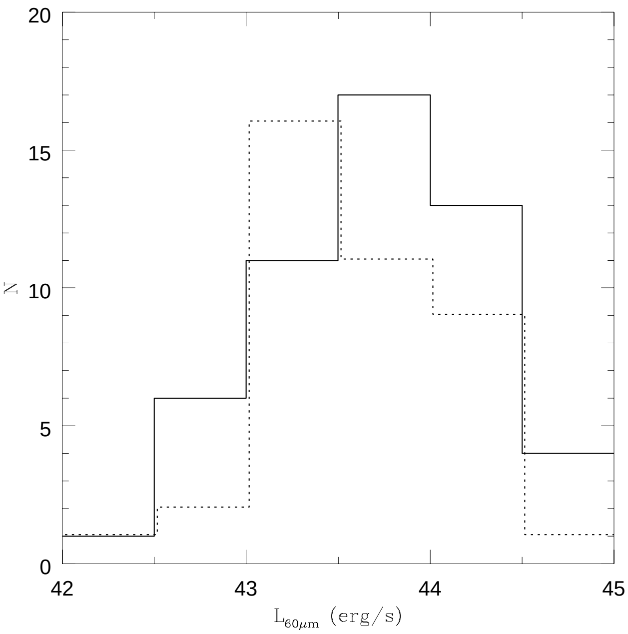

FIG. 1.—Comparison of the 60 μm luminosity of Seyfert 1 (*dotted line*) and Seyfert 2 (*solid line*) galaxies.

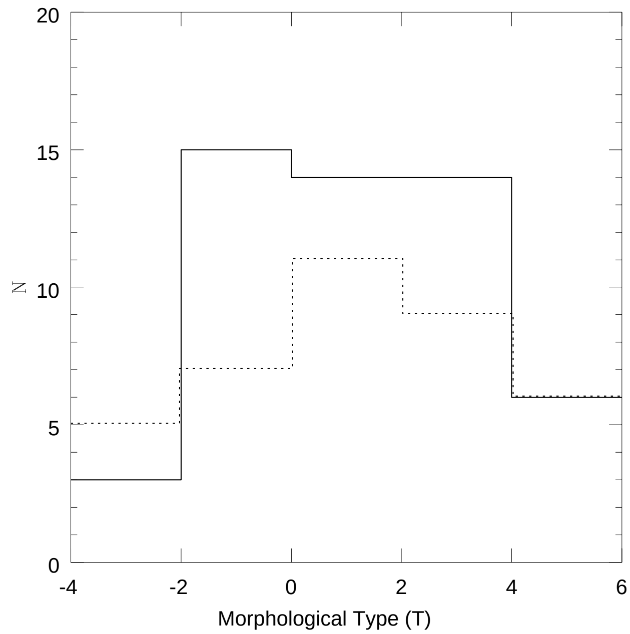

FIG. 2.—Comparison of the morphological types of the host galaxies of Seyfert 1 (*dotted line*) and Seyfert 2 (*solid line*) galaxies.

tion objects. Figure 2 shows the distribution of morphological types; it can be seen that both groups have similar distributions, with the K-S test showing that two samples drawn from the same parent population would differ this much 99.86% of the time, or in other words, would be more alike only 0.14% of the time.

3. RESULTS

Figure 3 shows the histogram of [O II]/[Ne III], where it can be seen that Seyfert 1 galaxies have, on average, smaller values than Seyfert 2 galaxies, indicating a higher excitation spectrum. Of particular interest in this histogram is the double cutoff in the distribution; for [O II]/[Ne III] < 1 there are 12 Seyfert 1 and only two Seyfert 2 galaxies, while for values of [O II]/[Ne III] > 3.5 there are only Seyfert 2 galaxies. Table 3 shows the result of the K-S test for this emission-line ratio, which shows that two samples drawn from the same parent population would differ this much 0.02% of the time.

Figure 4 shows the histogram of [O II]/[Ne V]. As for [O II]/[Ne III], Seyfert 1 galaxies are again displaced toward values smaller than those found for Seyfert 2 galaxies. For [O II]/[Ne V] < 1, there are 17 Seyfert 1 galaxies and only one Seyfert 2 galaxy. However, for this line ratio, there is not a high cutoff value, above which only Seyfert 2 galaxies are found, as is the case for [O II]/[Ne III]. The K-S test shows that two samples drawn from the same parent population would differ this much only 0.16% of the time. It should be noted that we only found [Ne V] fluxes for approximately 45% of the galaxies in the sample. This is in part because not all of the detectors have a good sensitivity below 3700 Å and because most of the NLR studies are centered on emission lines above 3700 Å. Care must also be taken when analyzing emission-line ratios involving [Ne V] because the detection of this line can be biased toward high-excitation objects.

Figure 5 shows the distribution of [Ne III]/[Ne V]. Apart from the fact that there are seven Seyfert 1 and no Seyfert 2

TABLE 3

COMPARISON BETWEEN SEYFERT 1 AND SEYFERT 2 GALAXIES

	Seyfert 1			Seyfert 2			
Ratio (1)	Measurements Available (2)	Mean (3)	Standard Deviation (4)	Measurements Available (5)	Mean (6)	Standard Deviation (7)	P (%) (8)
60 μm	40	43.61	0.48	52	43.71	0.60	43.74
Morphological Types	37	...	...	52	...	...	99.86
[O II]/[Ne III]	52	1.73	0.81	68	2.91	1.37	0.02
[O II]/[O III]	52	0.19	0.11	68	0.26	0.16	22.59
[O II]/[Ne V]	31	1.54	1.6	21	3.49	2.35	0.16
[Ne III]/[Ne V]	31	1.05	0.74	21	1.55	0.85	10.87

NOTE.—Col. (1): The quantity that is being analyzed; cols. (2) and (5): number of Seyfert 1 and Seyfert 2 galaxies with the measurement available; cols. (3) and (6): their average value; cols. (4) and (7): their standard deviation; col. (8): the K-S test probability of two samples drawn from the same parent population to differ this much.

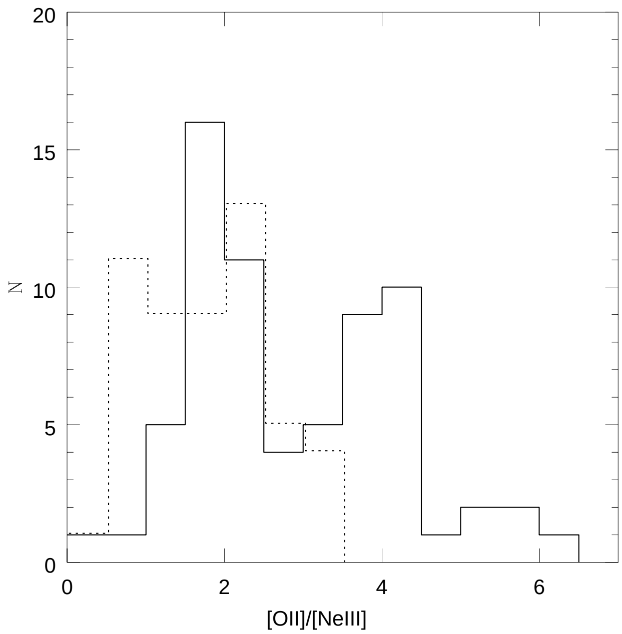

FIG. 3.—Comparison of the [O II]/[Ne III] distribution in Seyfert 1 (*dotted line*) and Seyfert 2 (*solid line*) galaxies.

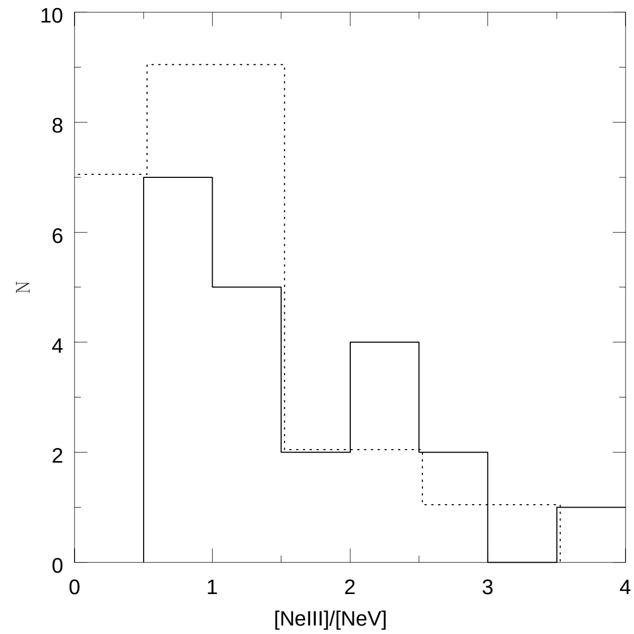

FIG. 5.—Comparison of the [Ne III]/[Ne V] distribution in Seyfert 1 (*dotted line*) and Seyfert 2 (*solid line*) galaxies.

galaxies with [Ne III]/[Ne V] < 0.5, the two distributions are approximately similar, the K-S test showing that two samples drawn from the same parent population would differ this much only 11% of the time. However, as stated above, this result should be taken with caution, since it includes the [Ne V] line.

The histogram of [O II]/[O III] is shown in Figure 6, where it can be seen that Seyfert 1 and Seyfert 2 galaxies have a similar distribution of values. The K-S test shows that two samples drawn from the same parent population would differ this much only 23% of the time. This emission-line ratio is shown here because it is one of the most common indicators of gas excitation. However, because of the large wavelength difference between the two lines (≈ 1300 Å), this ratio is extremely dependent on internal reddening; even the small internal reddening of $E(B-V) = 0.2$ increases the [O II]/[O III] ratio by $\approx 20\%$. As discussed above, [Ne III] originates in regions similar to [O III], and the [O II]/[Ne III] ratio can be substituted for [O II]/[O III].

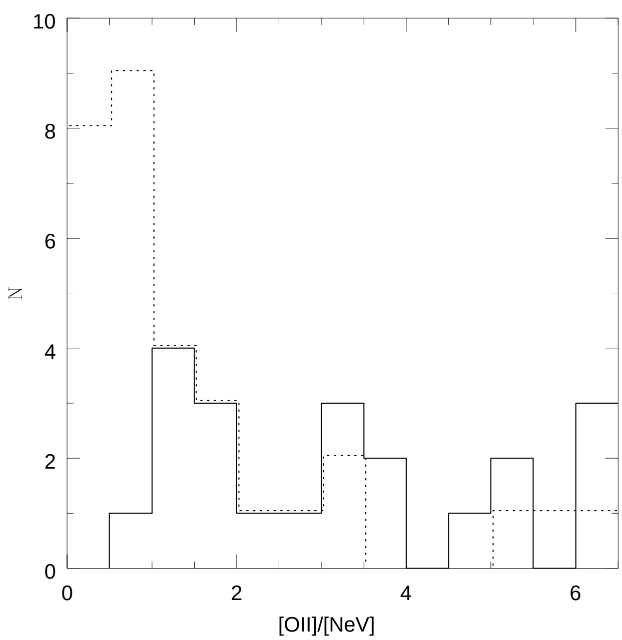

FIG. 4.—Comparison of the [O II]/[Ne V] distribution in Seyfert 1 (*dotted line*) and Seyfert 2 (*solid line*) galaxies.

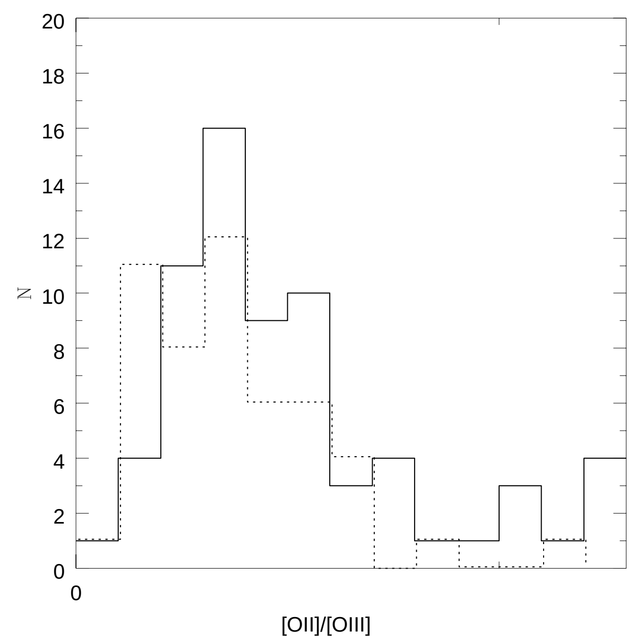

FIG. 6.—Comparison of the [O II]/[O III] distribution in Seyfert 1 (*dotted line*) and Seyfert 2 (*solid line*) galaxies.

4. DISCUSSION

4.1. *Photoionization Models*

The results presented in the previous section show that the average excitation of the NLRs of Seyfert 1 galaxies is larger than that for Seyfert 2 galaxies. This result is interpreted using diagnostic diagrams involving the emission-line ratios studied in this paper. Figures 7*a*, 7*b*, and 7*c* show the diagrams for log [O II]/[Ne V] × log [O II]/[Ne III], log [Ne III]/[Ne V] × log [O II]/[Ne III], and log [O II]/[O III] × log [O II]/[Ne III], respectively. It can be seen that Seyfert 1 galaxies are more concentrated toward the lower left-hand side in these diagrams, which corresponds to a higher excitation, confirming the results

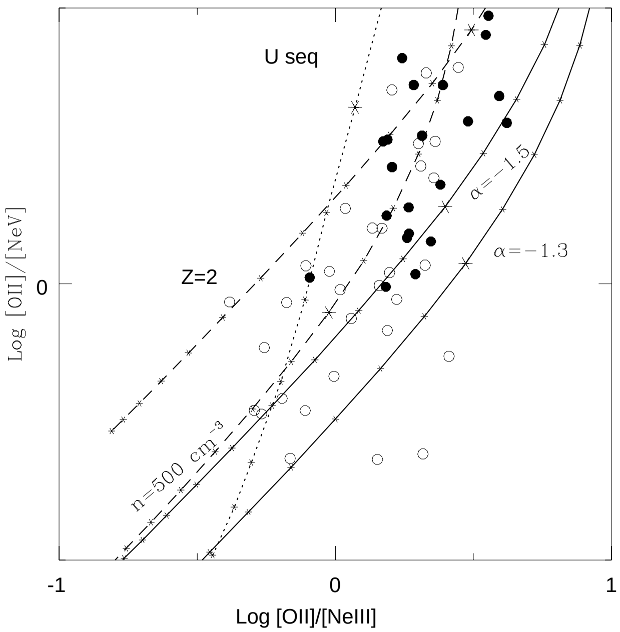

FIG. 7*a*

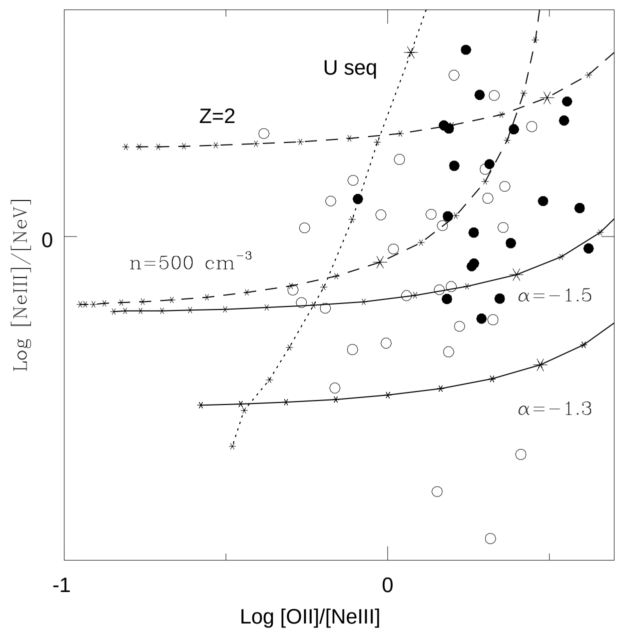

FIG. 7*b*

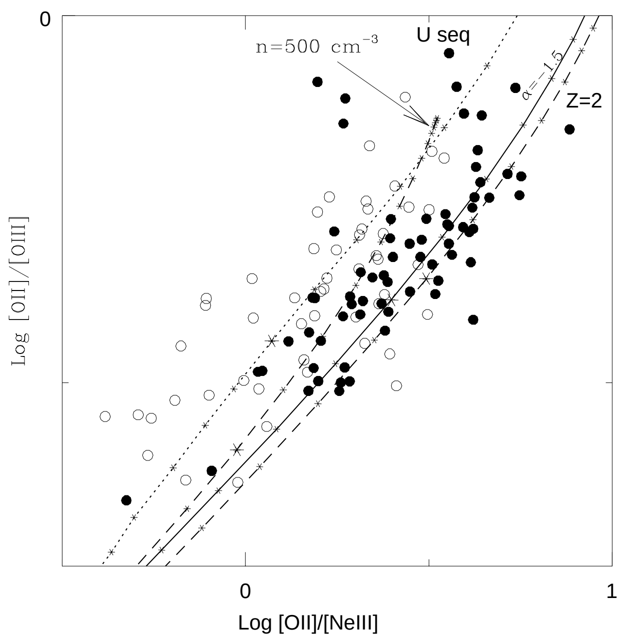

FIG. 7*c*

FIG. 7.—(*a*) Comparison of the emission-line ratios, log [O II]/[Ne V] × log [O II]/[Ne III], and photoionization models. Open circles show Seyfert 1 galaxies; filled circles show Seyfert 2 galaxies. The solid lines show the $A_{M/I}$ sequences of models with $n = 50$ cm^{-3}, $Z = 1$, ionized by a power-law continuum with slope $\alpha = -1.3$ or $\alpha = -1.5$, as indicated beside the line. The dashed lines show the $A_{M/I}$ sequences of models ionized by power-law spectra with $\alpha = -1.5$, but $n = 500$ cm^{-3} and $Z = 1$, or $n = 50$ cm^{-3} and $Z = 2$, as indicated beside the line by $n = 500$ cm^{-3} and $Z = 2$, respectively. $A_{M/I}$ was varied in the range $0.01 \leq A_{M/I} \leq 634$ in steps of 0.2 dex and decreases from left to right in the plot. The asterisks along the lines are separated by 0.2 dex, and the large asterisk corresponds to $A_{M/I} = 4$. The dotted line shows the sequence of ionization parameter models, calculated using a power-law ionizing spectrum with $\alpha = -1.3$, $n = 50$ cm^{-3}, and $Z = 1$. U was varied in the range $-4 \leq \log U \leq -0.8$ in steps of 0.2 dex. The asterisks along the line are separated by 0.2 dex, with the large asterisk corresponding to $\log U = -2$. (*b*) Same as (*a*), for the diagram log [Ne III]/[Ne V] × log [O II]/[Ne III]. (*c*) Same as (*a*), for the diagram log [O II]/[O III] × log [O II]/[Ne III]. Because the models with $\alpha = -1.3$ and $\alpha = -1.5$ are very similar, the plot only shows the models with $\alpha = -1.5$.

obtained from Figures 3, 4, 5, and 6. These distributions of emission-line ratios are compared with photoionization models in order to analyze the possible origins of this difference in excitation.

These results can be interpreted from the point of view of models that combine different proportions of matter and ionization-bounded clouds. In these models, the matter-bounded clouds produce most of the high-excitation lines ([Ne III], [O III], and [Ne V]) and few low-excitation lines ([O II] and [N II]), while the ionization-bounded clouds produce most of the low-ionization lines and few high-excitation lines. The use of such models was proposed by Viegas & Prieto (1992) to explain the emission-line region of 3C 227. Later, Binette, Wilson, & Storchi-Bergmann (1996; hereafter, BWSB96) used models of this kind to study the extended NLRs of Seyfert galaxies, showing their efficacy in reproducing high-excitation lines such as [Ne V] $\lambda3426$ and He II $\lambda4686$ as well as the [O III] temperature, which has always been a problem for the traditional photoionization models based on sequences of ionization parameters.

Sequences of models, adding different proportions of matter and ionization-bounded clouds, were calculated using the photoionization code MAPPINGS (Binette et al. 1993a, 1993b), following the description given in BWSB96. The models were calculated using a power-law ionizing spectrum of the form $F_\nu \propto \nu^\alpha$; two different values of α were tested, -1.3 and -1.5. The matter-bounded clouds are ionized by this spectrum, and the calculation stops when 40% of the incident spectrum is absorbed. The output-reprocessed spectrum from the matter-bounded clouds is what ionizes the ionization-bounded clouds. The models also assume that the ionization-bounded clouds leak some of the input radiation, in order to avoid overproduction of low-ionization lines such as [O II] and [N II]. In the case of $\alpha = -1.3$, it is assumed that the ionization-bounded clouds allow 3% of the ionizing radiation to escape, while for $\alpha = -1.5$ this value is 10%.

The models were calculated considering an isobaric prescription, in which the pressure is constant within any matter- or ionization-bounded cloud. The ionization parameter adopted for the matter-bounded spectrum was $U = 0.04$. Nevertheless, for the ionization-bounded clouds of the $A_{M/I}$ sequence (see below), instead of specifying the ionization parameter, the pressure was fixed at 20 times that of the matter-bounded clouds, following BWSB96. The adopted density was $n = 50$ cm^{-3}, and the gas metal abundance was solar ($Z = 1$). It is also assumed that the gas is mixed with a small quantity of dust, $\mu = 0.015$,[2] and that the abundance of metals in the grains is depleted from the gas. Note that this is a very small amount of dust; according to BWSB96, higher amounts of dust produce only minimal changes in the output spectrum of ionization-bounded clouds, but can have larger effects on the matter-bounded clouds. However, the matter-bounded clouds are not expected to have large quantities of dust, since dust can be easily destroyed by the radiation field. The only independent parameter in these models is the ratio of the solid angle subtended by matter-bounded clouds to the solid angle subtended by ionization-bounded clouds ($A_{M/I}$). Larger values correspond to a larger contribution from matter-bounded clouds relative to ionization-bounded clouds and vice versa. This parameter was varied in the range $0.01 \leq A_{M/I} \leq 634$, in steps of 0.2 dex. These models are shown as a solid line in Figures 7*a*, 7*b*, and 7*c*, with the value of α indicated beside the line.

In order to test the effects of other physical and chemical conditions, two other sequences of $A_{M/I}$ models were calculated. In the first set of models, $\alpha = -1.5$, with the same parameters as above but for gas with twice the solar metallicity ($Z = 2$). In the second set of models, $\alpha = -1.5$ and $Z = 1$, but the density is 500 cm^{-3}. These models have the same range of $A_{M/I}$ as above and are shown as long-dashed lines in Figures 7*a*, 7*b*, and 7*c*, identified as $Z = 2$ and $n = 500$ cm^{-3}, respectively.

Just for comparison with the above models, MAPPINGS was also used to calculate traditional sequences of models, varying only the ionization parameter. The parameters of these models were a power-law ionizing spectrum with $\alpha = -1.3$, constant density $n = 50$ cm^{-3}, metallicity $Z = 1$, and dust content $\mu = 0.015$. As for the $A_{M/I}$ models, two other sequences, one with $n = 500$ cm^{-3} and $Z = 1$, the other with $n = 50$ cm^{-3} and $Z = 2$, were also tried. It was assumed that 3% of the ionizing radiation escapes from the clouds, in order to avoid the overproduction of low-ionization lines. The ionization parameter was varied in the range $-4 \leq \log U \leq -0.8$, in steps of 0.2 dex. The three sequences of models are very similar, the only exception being the sequence of models with $Z = 2$ in the diagram log ([O II]/[O III]) × log ([O II]/[Ne III]) (Fig. 7*c*), which are very similar to the $A_{M/I}$ sequence with $Z = 2$. Because of this, only the sequence with $n = 50$ cm^{-3} and $Z = 1$ is presented as a dotted line in Figures 7*a*, 7*b*, and 7*c*.

It can be seen in Figures 7*a* and 7*b* that the $A_{M/I}$ sequences of models cover very well the observed distribution of values. In the case of Figure 7*c*, showing the diagram of log ([O II]/[O III]) × log ([O II]/[Ne III]), these models have some problems in reproducing the observed distribution of values. It would be necessary to change other parameters, such as the amount of dust in the models, the pressure jump between the matter and the ionization-bounded clouds, or the amount of radiation that leaks from the ionization-bounded clouds in order to better reproduce the observed distribution of values. The fact that Seyfert 1 galaxies have [O II]/[Ne III] and [O II]/[Ne V] values smaller than those of Seyfert 2 galaxies can be interpreted as an effect of the smaller contribution from ionization-bounded clouds relative to matter-bounded clouds in the spectra of those objects. This comparison also shows that the $A_{M/I}$ models with $\alpha = -1.3$ are not as good a representation for the observed values as the ones with $\alpha = -1.5$ because they produce too large fluxes of the higher excitation lines, such as [Ne V].

A comparison with the traditional U sequence of models shows that they are a poor representation of the data points, even varying parameters such as the gas abundance or density. Only in Figure 7*c*, where the $A_{M/I}$ sequence of models has some problems in representing the observed distribution of points, could these models be a better representation for the data. However, they require unconventionally large ionization parameters ($U > 0.01$).

4.2. *Possible Interpretations*

Four possible interpretations of the above result are studied here.

[2] The quantity μ is the dust-to-gas ratio of the clouds, in units of the solar neighborhood dust-to-gas ratio.

1. *Some of the matter-bounded clouds (which produce most of the* [Ne III], [O III], *and* [Ne V]) *are hidden by the circumnuclear torus in Seyfert 2 galaxies.* A similar problem was found by Jackson & Browne (1990) in their comparison of quasars with radio galaxies. They show that the [O III] emission of quasars is much stronger than that of radio galaxies, proposing that part of the [O III] emission is obscured by the torus in the latter objects. Hes, Barthel, & Fosbury (1993) showed that when comparing the [O II] emission of quasars and radio galaxies, which originates in less obscured, lower excitation regions, both classes of objects have very similar distributions, corroborating the obscuration scenario.

While the obscuration scenario may be the solution for radio galaxies and quasars, it may not be the general case for Seyfert 2 galaxies. Assuming that the [O II] emission in Seyfert 2 galaxies is similar to that of Seyfert 1 galaxies and that it is not blocked by the torus, we can calculate, using the average values given in Table 3, that $\approx$40% of the [Ne III] emission, $\approx$55% of the [Ne V] emission, and $\approx$25% of the [O III] emission should be blocked by the torus in Seyfert 2 galaxies. This could happen for some of the Seyfert 2 galaxies in the sample, but note that these are large values and go against the fact that Seyfert 2 galaxies have lower excitation lines (like [O II]) that are more luminous than those of Seyfert 1 galaxies of similar optical luminosity (Yee 1980; Shuder 1980). In addition, Seyfert 2 galaxies usually have extended NLRs (Pogge 1989; Schmitt & Kinney 1996). Another fact that goes against the obscuration scenario being the general case is that if part of the high-excitation emission line region is hidden by the torus, we would expect to see considerable amounts of polarized [O III] emission in Seyfert 2 galaxies. As shown by Goodrich (1992), with a small number of exceptions, Seyfert 2 galaxies do not have high degrees of polarized [O III] emission.

2. *We see a smaller number of ionization-bounded clouds in Seyfert 1 galaxies because they are seen from the back and are extincted.* Since the ionization-bounded clouds are responsible for most of the [O II] emission and very little of the [Ne III], [Ne V], and [O III], this would imply a reduction of the ratios [O II]/[Ne III], [O II]/[Ne V], and [O II]/[O III] in Seyfert 1 relative to Seyfert 2 galaxies.

From an analysis of the X-ray spectra of Seyfert 1 galaxies (Reynolds 1997; Weaver, Arnaud, & Mushotzky 1995), it is known that they usually have small column densities of absorbing material ($N_{\rm H\,I} < 10^{21}$ cm^{-2}). Assuming a standard dust-to-gas ratio ($A_V = 5 \times 10^{-22} N_{\rm H\,I}$), it is possible to estimate a typical value of extinction from the above $N_{\rm H\,I}$, which is $A_V < 0.5$ [$E(B-V) \approx 0.2$]. In the case of $E(B-V) = 0.1$, the [O II] emission of the ionization-bounded clouds would be reduced by $\approx$35%, which could explain the difference between Seyfert 1 and Seyfert 2 galaxies. However, this scenario only works when the ionization-bounded clouds do not block the direct view of the matter-bounded clouds; otherwise, the high-excitation lines would also be obscured.

3. *There is a smaller number of ionization-bounded clouds in Seyfert 1 galaxies, possibly because of the orientation of the circumnuclear torus relative to the galaxy plane.* In this scenario, Seyfert 1 galaxies have their circumnuclear torus axis preferentially aligned closer to the host galaxy plane axis, while in Seyfert 2 galaxies the torus can have any orientation. In this way, Seyfert 1 galaxies would have smaller NLRs because their ionizing radiation would shine out of the galaxy disk and find only a small number of clouds to be ionized, thus resulting in a smaller number of ionization-bounded clouds in these objects. On the other hand, since the Seyfert 2 galaxy torus axis can have any orientation relative to the host galaxy disk, there is a larger chance for the ionizing radiation to cross the galaxy disk in these objects, which would result in more gas clouds to be ionized. The clouds closer to the nucleus filter the ionizing radiation, and the more distant clouds are ionized only by this fainter and filtered continuum. Because of the larger number of clouds along the disk, the nuclear radiation ionizes a larger number of clouds, and the effect is similar to seeing a larger number of ionization-bounded clouds in Seyfert 2 galaxies.

Some of the results available in the literature, discussed in the introduction, corroborate this scenario. Seyfert 1 galaxies have higher [O III] $\lambda4363/\lambda5007$ ratios than Seyfert 2 galaxies, which could be explained as the result of higher [O III] temperatures or higher densities. If the higher [O III] $\lambda4363/\lambda5007$ ratios of Seyfert 1 galaxies are in fact due to a higher [O III] temperature, this is consistent with a smaller proportion of ionization-bounded clouds in these objects, as shown by the models of BWSB96. This interpretation can also explain the results obtained by Schmitt & Kinney (1996), that Seyfert 1 galaxies have much smaller NLRs than Seyfert 2 galaxies (when they are compared in a similar way, as if they were seen pole-on). Kraemer et al. (1998) confirmed this in the individual case of the Seyfert 1 galaxy NGC 5548, showing that this galaxy has a compact NLR, on the order of 70 pc.

The above results imply that the NLRs of Seyfert 1 galaxies have less gas than the NLRs of Seyfert 2 galaxies, which can be explained if the Seyfert 1 torus axis is aligned closer to the host galaxy plane axis. This scenario is supported by the observation of the absence of Seyfert 1 galaxies in edge-on galaxies (Keel 1980; Maiolino & Rieke 1995; Simcoe et al. 1997) and by the relative orientation between linear radio structures and the host galaxy major axis in Seyfert 1 galaxies (Schmitt et al. 1997).

4. *Seyfert 2 galaxies are more strongly associated with circumnuclear star formation (high-metallicity* H II *regions) than are Seyfert 1 galaxies.* Since high-metallicity H II regions are strong emitters of [O II] and weak emitters of [Ne III], if the nuclear emission of Seyfert 2 galaxies is more likely to be mixed with H II regions than Seyfert 1 galaxies, this would explain the fact that their NLRs show less excited gas. Some evidence for the existence of circumnuclear star-forming regions in Seyfert 2 galaxies is given by Heckman et al. (1995, 1997) and Thuan (1984). However, this evidence is restricted to a small number of galaxies, and it would be necessary to study the stellar population of a complete sample of Seyfert 1 and Seyfert 2 galaxies to see if there is any difference between these two classes of objects and to confirm whether Seyfert 2 galaxies in fact have more circumnuclear star formation. One such attempt was made by Schmitt, Storchi-Bergmann, & Cid Fernandes (1998), who synthesized the nuclear stellar population of 20 Seyfert 2 galaxies, showing that young stars usually contribute less than 5% (less than 1% in more than 50% of the sample) of the light of these galaxies at 5870 Å.

5. SUMMARY

This paper follows from a literature search of the fluxes of the emission lines [O II], [Ne III], [Ne V], and [O III] and of the 60 μm continuum for a sample of 52 Seyfert 1 and 68 Seyfert 2 galaxies. The analysis of possible selection effects shows that the two groups are not biased with respect to morphological type, have similar values of 60 μm luminosity, and were observed with apertures of similar metric sizes.

A comparison of the distributions of the emission-line ratios [O II]/[Ne III] and [O II]/[Ne V] in Seyfert 1 and Seyfert 2 galaxies shows that the two groups are considerably different, with the Seyfert 2 spectra presenting more low-excitation emission than the spectra of Seyfert 1 galaxies. The emission-line ratios are compared to sequences of models in which only the ionization parameter varies, as well as with models that combine different proportions of matter and ionization-bounded clouds. It is shown that the distribution of observed points can be better represented by the latter models, with Seyfert 1 galaxies having a smaller number of ionization-bounded clouds than Seyfert 2 galaxies.

Four possible interpretations for this difference are proposed. The most likely explanation is that Seyfert 1 galaxies have smaller NLRs and thus a smaller number of ionization-bounded clouds. The NLRs of Seyfert 1 galaxies could be smaller than those of Seyfert 2 galaxies as the result of an inclination effect. There is a growing quantity of evidence showing that the torus axis of Seyfert 1 galaxies is more likely to be aligned close to the galaxy plane axis, while in Seyfert 2 galaxies it can have any direction (Schmitt et al. 1997; Simcoe et al. 1997). In this way, the amount of gas ionized by the nuclear radiation would be smaller in Seyfert 1 than in Seyfert 2 galaxies, resulting in a larger number of ionization-bounded clouds in these objects.

Two possibilities assume that a portion of the matter-bounded clouds are hidden by the circumnuclear torus in Seyfert 2 galaxies or that the ionization-bounded clouds are seen from the back in Seyfert 1 galaxies, creating the impression that Seyfert 1 galaxies are more excited than Seyfert 2 galaxies. The evidence presented above goes against these two scenarios as a general case. However, it is not possible to rule out individual cases in which this could happen.

A fourth possibility assumes that Seyfert 2 galaxies have a larger number of circumnuclear star-forming regions than Seyfert 1 galaxies. There is some evidence of circumnuclear star formation in some Seyfert 2 galaxies. However, it should still be determined whether this happens for all Seyfert 2 galaxies and whether there is a difference between the stellar populations of the two types of Seyferts.

It should be noted that the results presented in this paper were obtained from a sample selected from the literature, rather than a sample selected from an isotropic property. Although it was shown that the two samples have similar intrinsic properties, there could still be some selection effects affecting the results. In order to avoid these, it would be important to test these results using homogeneous measurements of a sample selected by an isotropic property.

I would like to thank R. Antonucci, L. Binette, A. Kinney, T. Storchi-Bergmann, C. Winge, and the anonymous referee for useful comments and suggestions. L. Binette is also thanked for making available the code MAPPINGS. This research has made use of the NASA/IPAC Extragalactic Database (NED), which is operated by the Jet Propulsion Laboratory, Caltech, under contract to NASA.

REFERENCES

Alloin, D., Bica, E., Bonatto, C. J., & Prugniel, P. 1992, A&A, 266, 117
Alloin, D., Pelat, D., Phillips, M., & Whittle, M. 1985, ApJ, 288, 205
Anderson, K. S. 1970, ApJ, 162, 743
Antonucci, R. R. J., & Miller, J. S. 1985, ApJ, 297, 621
Baldwin, J. A., Phillips, M. M., & Terlevich, R. 1981, PASP, 93, 5
Binette, L., Wang, J. C. L., Villar-Martín, M., Martin, P. G., & Magris, C. M. 1993a, ApJ, 414, 535
Binette, L., Wang, J. C. L., Zuo, L., & Magris, C. M. 1993b, AJ, 105, 797
Binette, L., Wilson, A. S., & Storchi-Bergmann, T. 1996, A&A, 312, 365 (BWSB96)
Boksenberg, A., Shortridge, K., Allen, D. A., Fosbury, R. A. E., Penston, M. V., & Savage, A. 1975, MNRAS, 173, 381
Cohen, R. D. 1983, ApJ, 273, 489
De Robertis, M. M., & Osterbrock, D. E. 1986, ApJ, 301, 727
de Vaucouleurs, G., de Vaucouleurs, A., Corwin, H. G., Jr., Buta, R. J., Paturel, G., & Fouque, P. 1991, Third Reference Catalogue of Bright Galaxies (New York: Springer)
Diaz, A. I., Prieto, M. A., & Wamsteker, W. 1988, A&A, 195, 53
Durret, F., & Bergeron, J. 1986, A&A, 156, 51
———. 1988, A&AS, 75, 273
Ferland, G. J., & Osterbrock, D. E. 1986, ApJ, 318, 145
Gallimore, J. F., Baum, S. A., O'Dea, C. P., Brinks, E., & Pedlar, A. 1996, ApJ, 462, 740
Gonzalez Delgado, R. M., & Perez, E. 1996, MNRAS, 280, 53
Goodrich, R. W. 1992, ApJ, 399, 50
Goodrich, R. W., & Osterbrock, D. E. 1983, ApJ, 269, 416
Greenhill, L. J., Gwinn, C. R., Antonucci, R., & Barvainis, R. 1996, ApJ, 472, 21
Heckman, T. M., & Balick, B. 1979, A&A, 79, 350
Heckman, T. M., et al. 1995, ApJ, 452, 549
———. 1997, ApJ, 482, 114
Hes, R., Barthel, P. D., & Fosbury, R. A. E. 1993, Nature, 362, 326
Jackson, N., & Browne, I. W. A. 1990, Nature, 343, 43
Kay, L. 1994, ApJ, 430, 196
Keel, W. C. 1980, AJ, 85, 198
Koski, A. T. 1978, ApJ, 223, 56
Kraemer, S. B., Crenshaw, D. M., Filippenko, A. V., & Peterson, B. M. 1998, ApJ, 499, 719
Kunth, D., Sargent, W. L. W., & Bothum, G. D. 1987, AJ, 93, 29
Lipari, S., Tsvetanov, Z., & Macchetto, F. 1993, ApJ, 405, 186
Maiolino, R., & Rieke, G. H. 1995, ApJ, 454, 95
Miller, J. S., & Goodrich, R. W. 1990, ApJ, 355, 456
Miyoshi, M., Moran, J., Herrnstein, J., Greenhill, L., Nakai, N., Diamond, P., & Inoue, M. 1995, Nature, 373, 127
Moran, E. C., Halpern, J. P., Bothum, G. D., & Becker, R. H. 1992, AJ, 104, 990
Morris, S. L., & Ward, M. J. 1988, MNRAS, 230, 639
Mulchaey, J. S. 1994, Ph.D. thesis, Univ. Maryland
Mulchaey, J. S., Mushotzky, R. F., & Weaver, K. A. 1992, ApJ, 390, L69
Osterbrock, D. E. 1981, ApJ, 249, 462
———. 1985, PASP, 97, 25
Osterbrock, D. E., & Dahari, O. 1983, ApJ, 273, 478
Osterbrock, D. E., & Pogge, R. W. 1985, ApJ, 297, 166
Phillips, M. M., Charles, P. A., & Baldwin, J. A. 1983, ApJ, 266, 485
Pier, E. A., & Krolik, J. H. 1992, ApJ, 401, 99
Pogge, R. W. 1988a, ApJ, 328, 519
———. 1988b, ApJ, 332, 702
———. 1989, ApJ, 345, 730
Reynolds, C. S. 1997, MNRAS, 286, 513
Rodriguez-Ardila, A., Pastoriza, M. G., Bica, E., & Maza, J. 1996, ApJ, 463, 522
Rola, C. S., Terlevich, E., & Terlevich, R. J. 1997, MNRAS, 289, 419
Schmitt, H. R., & Kinney, A. L. 1996, ApJ, 463, 498
Schmitt, H. R., Kinney, A. L., Storchi-Bergmann, T., & Antonucci, R. 1997, ApJ, 477, 623
Schmitt, H. R., & Storchi-Bergmann, T. 1995, MNRAS, 276, 592
Schmitt, H. R., Storchi-Bergmann, T., & Baldwin, J. A. 1994, ApJ, 423, 237
Schmitt, H. R., Storchi-Bergmann, T., & Cid Fernandes, R. 1998, in preparation
Shuder, J. M. 1980, ApJ, 240, 32
Shuder, J. M., & Osterbrock, D. E. 1981, ApJ, 250, 55
Simcoe, R., McLeod, K. K., Schachter, J., & Elvis, M. 1997, ApJ, 489, 615

Storchi-Bergmann, T., Bica, E., & Pastoriza, M. G. 1990, MNRAS, 245, 749
Storchi-Bergmann, T., & Pastoriza, M. G. 1989, ApJ, 347, 195
Terlevich, R., Melnick, J., Masegosa, J., Moles, M., & Copetti, M. V. F. 1991, A&AS, 91, 285
Thuan, T. X. 1984, ApJ, 281, 126
Tran, H. 1995, ApJ, 440, 565
Ulvestad, J. S., & Wilson, A. S. 1983, AJ, 88, 253
———. 1984a, ApJ, 278, 544
Ulvestad, J. S., & Wilson, A. S. 1984b, ApJ, 285, 439
———. 1989, ApJ, 343, 659
Viegas, S. M., & Prieto, M. A. 1992, MNRAS, 258, 483
Ward, M., Penston, M. V., Blades, J. C., & Turtle, A. J. 1980, MNRAS, 193, 563
Weaver, K. A., Arnaud, K. A., & Mushotzky, R. F. 1995, ApJ, 447, 121
Wilson, A. S., & Penston, M. V. 1979, ApJ, 232, 389
Yee, H. K. C. 1980, ApJ, 241, 894